Astron. Astrophys. 315, L313–L316 (1996)

ASTRONOMY AND ASTROPHYSICS

Very small grain emission in NGC 7023⋆

R.J. Laureijs[1], **J. Acosta-Pulido**[5,1,2], **P. Ábráham**[6,5], **U. Kinkel**[5,1], **U. Klaas**[5,1], **H.O. Castaneda**[5,1,2], **L. Cornwall**[3,1], **C. Gabriel**[1], **I. Heinrichsen**[4,1], **D. Lemke**[5], **G. Pelz**[5,1], **B. Schulz**[1], **and H.J. Walker**[3]

[1] ISO Science Operations Centre, Astrophysics Division of ESA, Villafranca, Apdo 50727, E-28080 Madrid, Spain
[2] IAC, E-38200 La Laguna, Tenerife, Spain
[3] CCLRC, Rutherford Appleton Laboratory, Chilton, Didcot, Oxon OX11 0QX, UK
[4] MPIK, Saupfercheckweg 1, D-69117, Heidelberg, Germany
[5] MPIA, Königstuhl 17, D-69117, Heidelberg, Germany
[6] Konkoly Observatory of the Hungarian Academy of Sciences, P.O. Box 67, H-1525 Budapest, Hungary

Received 29 July 1996 / Accepted 28 August 1996

Abstract. We observed the reflection nebula NGC7023 at various positions using wide and narrow band photometry centred on the 7.7 and 11.3 μm PAH emission features and wide band photometry at 20 and 25 μm. No significant variations have been detected over the nebula in the 7.3 and 20 μm continuum relative to the total emission in the 6-15 μm range (hereafter Γ). This result supports the hypothesis that most of the continuum emission in both bands come from very small grains.

In contrast, the 7.7 and 11.3 μm PAH emission features show clear variations. We find that in weaker radiation fields of the nebula the 11.3 and 7.7 μm features are not the dominant emission components in the 6-15 μm range. The 11.5 μm band increases whereas the 11.3 μm emission feature decreases relative to Γ in the outer parts of the nebula. The effect can be explained by increased hydrogenation of PAH molecules.

Key words: interstellar medium: reflection nebulae: NGC 7023 – interstellar medium: dust, extinction – interstellar medium: molecules

1. Introduction

The reflection nebula NGC 7023 was one of the first objects where direct evidence was found for the existence of very small dust particles with sizes of order 0.001 μm (Sellgren 1984). The observations by Sellgren et al. (1985) suggested that as well as the unidentified infrared bands (prominent at 3.3, 6.2, 7.7 and 11.3 μm) there must be a continuum in the 2-13 μm range due to transient heating of very small grains. To date, the infrared emission in the bands has been attributed to specific CC stretching and C-H bending modes of forms of polycyclic aromatic hydrocarbons (PAH's, Léger at al. 1989).

Despite all observational evidence the small grain emission is still not well understood, especially the distinction between PAH's supposedly emitting exclusively in bands and very small grains which should give rise to continuum in the 2-80 μm range (e.g. Puget and Léger, 1989).

In this letter we present ISOPHOT (Lemke et al. 1996) observations of NGC 7023 in the 6-30 μm range where the emission is expected to be dominated by very small dust particles. The PAH band emission as opposed to the continuum emission is investigated by observing in the dedicated ISOPHOT filters.

Table 1. Observed positions in NGC 7023, R.A in h,m,s, and Dec. in $^\circ\ '\ ''$ (Epoch 1950)

Pos.	R.A.	Dec.	Pos.	R.A.	Dec.
1	21 01 42.8	67 57 15	6	21 00 58.4	67 57 15
2	21 01 32.1	67 58 15	7	21 00 47.7	67 58 15
3	21 01 15.0	67 57 15	8	21 00 58.4	67 59 15
4	21 01 32.1	67 56 15	9	21 00 58.4	67 58 15
5	21 01 32.1	67 57 15			

2. Infrared observations and data processing

We selected 9 positions based on far-infrared maps presented by Casey (1991) which delineate the distribution of the large dust grains in the nebula (Table 1). The sequence is according to increasing far-infrared surface brightness (Fig. 1). Positions 5 and 9 are listed as IRAS 12 μm point sources.

Using sparse map AOTs PHT17, PHT18, and PHT19 (Klaas et al., 1994) we observed each position with the 7.3, 7.7, 11.3,

Send offprint requests to: R.J. Laureijs

⋆ Based on observations made with ISO, an ESA project with instruments funded by ESA Member States (especially the PI countries: France, Germany, the Netherlands and the United Kingdom) and with the participation of ISAS and NASA.

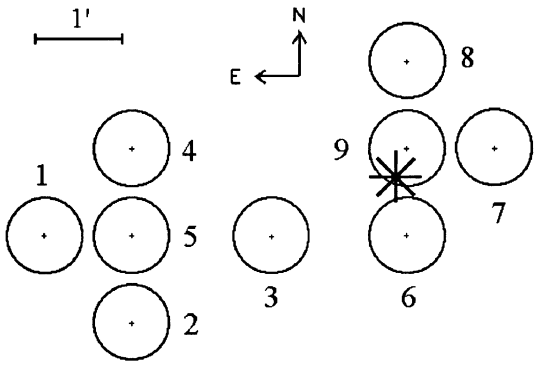

Fig. 1. Sparse map pointings in NGC7023. The position of the exciting star HD200775 is indicated by the star, the numbers refer to the positions in Table 1

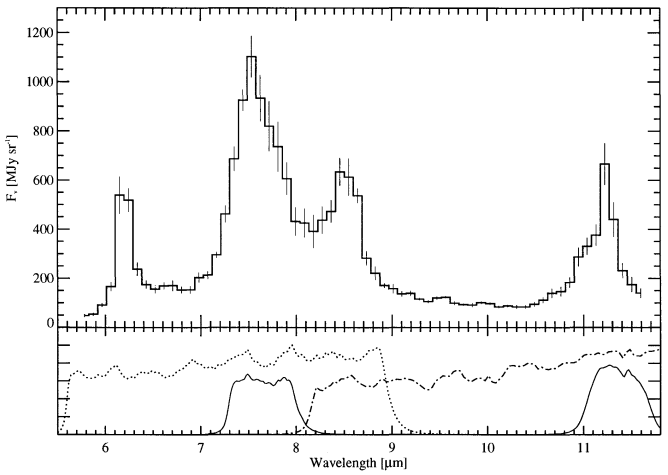

Fig. 2. Upper panel: PHT-S spectrum obtained at pos. 9, **lower panel**: the P_7.3 (dot), P_7.7 (solid), P_11.3 (solid) and P_11.5 (dash-dot) spectral response functions

and 11.5 μm filters of the P1 detector and the 20 and 25 μm filters of the P2 detector. In all cases the $52''$ aperture was used with 32 s integration time.

The first and last observations in each sparse map sequence of a given detector were followed by a measurement with the ISOPHOT internal fine calibration source (FCS). The signal stability of these FCS measurements confirmed that default responsivities for the P1 and P2 detectors can be used. We applied responsivities of 1.05 and 0.46 A/W, respectively. These values were obtained by standard observations of calibration stars.

The uncertainty in the filter measurements is dominated by short term detector drifts. These are minimized by adopting a pointing sequence where the expected power on the detector steadily increases. Although we made a correction for these drifts, we estimate a measurement to measurement uncertainty of 5%. We have used this number to calculate the uncertainties in the derived values.

However, currently the main sources of uncertainty in the photometry are systematic: (1) the relative system response among the filters are uncertain by up to 10%, and (2) the uncertainty in detector responsivity which is approximately 10%.

We corrected the derived surface brightness values for zodiacal emission by subtracting interpolated COBE values. As these data are collected at a different epoch with a different resolution we assumed an uncertainty of 20% for the background values.

The photometry with the 7.7 and 11.3 μm feature filters is complemented by a PHT-S spectrum taken at pos. 9. Observations of the calibration stars HR 6705 and HR 6688 were used to calibrate the spectrum with an absolute photometric accuracy of 30%.

3. Results

The PHT-S spectrum of NGC 7023 from 6-12 μm is displayed in Fig. 2. The results of the sparse map photometry are listed in Table 2. Except for the 11.3 μm filter, the surface brightness values from PHT-S photometry are in reasonable agreement with the PHT-P data (Table 2). The remaining discrepancies are probably due to the difference between the PHT-S and PHT-P apertures ($24'' \times 24''$ as opposed to $52''$), probing different emission regions.

Table 2. ISOPHOT photometry of NGC 7023 after background subtraction, all surface brightness values in MJy/sr. The surface brightness uncertainty before background correction is 5%. The first row gives the adopted background values. The last row lists the photometry obtained by integrating the PHT-S spectrum over the 7.3, 7.7, and 11.3 μm filterbands.

Pos.	$I_{7.7}$	$I_{7.3}$	$I_{11.3}$	$I_{11.5}$	I_{20}	I_{25}
I_{back}	2.8	2.8	14	14	21	24
1	39	20	46	38	43	41
2	79	38	93	57	63	89
3	76	37	92	52	78	102
4	101	48	143	68	88	125
5	132	61	192	86	112	152
6	300	117	326	112	150	247
7	400	161	474	150	204	320
8	202	67	347	99	170	254
9	1230	377	1240	402	782	1480
9 (PHT-S)	760	380	352			

To estimate the amount of PAH band versus continuum emission in the continuum filters we applied the following relationships:

$$P_c = \frac{P_{wide} - P_{narrow}}{\Delta\lambda_{wide} - \Delta\lambda_{narrow}} \Delta\lambda_{wide}, \quad (1)$$

and

$$P_l = \frac{P_{narrow}\Delta\lambda_{wide} - P_{wide}\Delta\lambda_{narrow}}{\Delta\lambda_{wide} - \Delta\lambda_{narrow}}, \quad (2)$$

where P_l and P_c are the powers in emission feature and continuum, respectively. The P_{wide}, P_{narrow}, $\Delta\lambda_{wide}$, and $\Delta\lambda_{narrow}$ are the in-band powers (= $\Delta\lambda I_\lambda$) and equivalenth

Table 3. Derived powers for emission feature and continuum in the 7.3 and 11.5 μm filterbands; Γ indicates the total power in the 7.3 plus 11.5 filters, all values in 10^{-6} W m^{-2}sr^{-1}

Pos.	$P_l(7.7)$	$P_c(7.3)$	$P_l(11.3)$	$P_c(11.5)$	Γ
1	0.97	2.72	0.23	5.07	9.0
2	2.09	5.02	0.78	7.00	15.0
3	2.05	4.74	0.95	6.31	14.1
4	2.76	6.15	1.73	7.68	18.3
5	3.69	7.67	2.42	9.57	23.3
6	9.70	12.0	4.78	10.8	37.3
7	12.7	17.1	7.22	13.5	50.5
8	7.23	5.19	5.49	8.24	26.2
9	45.7	24.0	18.8	37.1	126

widths of the wide band and narrow band filters that are centred on the same feature. In Table 3 we list the line and continuum fluxes derived according to Eqns. 1 and 2.

We define Γ as the sum of the in-band powers in the 7.3 and 11.5 μm filter bands. Since the wavelength range of the two filters are adjacent to each other, Γ should give an accurate estimate of the total energy emitted in the 6 - 15 μm wavelength range.

4. Analysis

The 7.3 μm filterband covers the wavelength interval 5.7-9.1 μm. From the PHT-S spectrum (Fig. 2) it can be seen that this filter covers three PAH features including the pedestal on which these are residing. The 11.3 μm feature appears isolated in the 9-11.6 μm region of the PHT-S spectrum. The 11.5 μm filterband covers the range 9.2-15 μm which is for a large part not covered by PHT-S.

To investigate the relative variation of the emission features over the nebula we present in Fig. 3 the ratio P_l/Γ for the 7.7 and 11.3 μm features as a function of Γ. Both features become relatively fainter towards lower Γ. The ratios $P_l(11.3)/\Gamma$ and $P_l(7.7)/\Gamma$ drop dramatically by factors of 3 and 2, respectively, towards lower Γ.

Similar relationships to those presented in Fig. 3 but for the continuum bands are presented in Fig. 4. Although the value of Γ varies by an order of magnitude, no obvious variation can be seen in the ratios $P_c(7.3)/\Gamma$ and $P_c(20)/\Gamma$. Most noticeable is a significant increase in $P_c(11.5)/\Gamma$ towards lower Γ. Excluding the uncertain position 1, the increase is about a factor 1.5 with respect to position 9.

Fig. 5 shows the ratios $P_l(11.3)/P_l(7.7)$ and $P_c(20)/P_c(25)$ as a function of Γ. The ratio $P_l(11.3)/P_l(7.7)$ increases with increasing Γ with an apparent maximum at Γ = 30 10^6 Wm^{-2}sr^{-1}. For higher Γ the ratio appears constant at about 0.5. The ratio $P_c(20)/P_c(25)$ shows marginal evidence for a systematic decrease towards high Γ. If the trend is real than it suggests that the colour temperature I_{20}/I_{25} *decreases* towards the centre of the nebula.

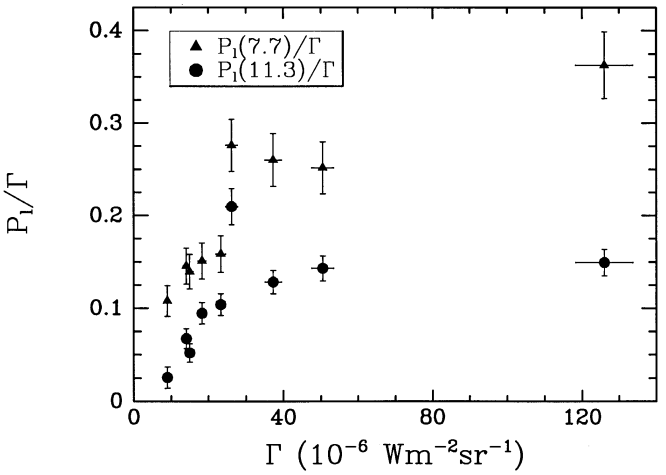

Fig. 3. Relative variation of the 7.7 and 11.3 μm emission features as a function of Γ. Γ increases towards the central star

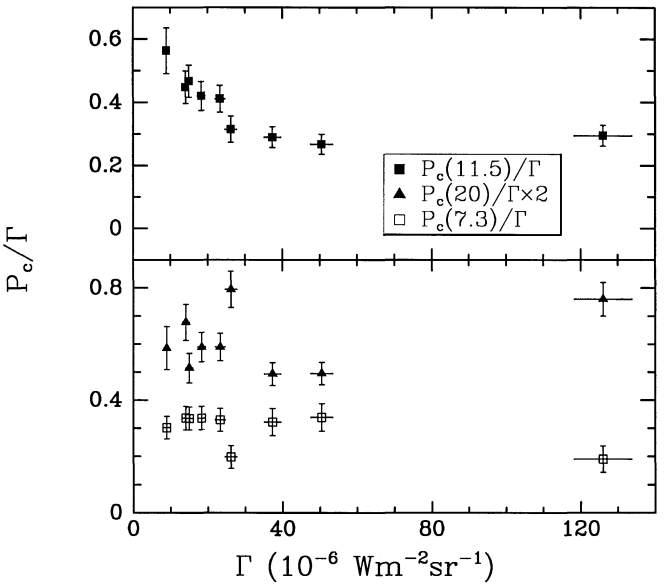

Fig. 4. The relationship between the relative continuum power in 3 bands and Γ

5. Discussion and conclusions

The presence of both decreasing as well as increasing trends in $I_c(11.5)/\Gamma$ and $P_l(11.3)/\Gamma$ rules out the possibility that the trends are due to instrumental artifacts. Both the 11.5 and 11.3 μm filters are using the same detector and both filter measurements were collected with the same measurement sequence at each position.

The absence of clear variations in $P_c(7.3)/\Gamma$ and $P_c(20)/\Gamma$ at different positions in the nebula (Fig. 4) supports the hypothesis that the continuum emission in the 7.3 and 20 μm bands is dominated by very small grains. The constant shape of the energy distribution at several positions in the nebula has also been observed by Sellgren (1984) from photometry in the 2-5 μm range.

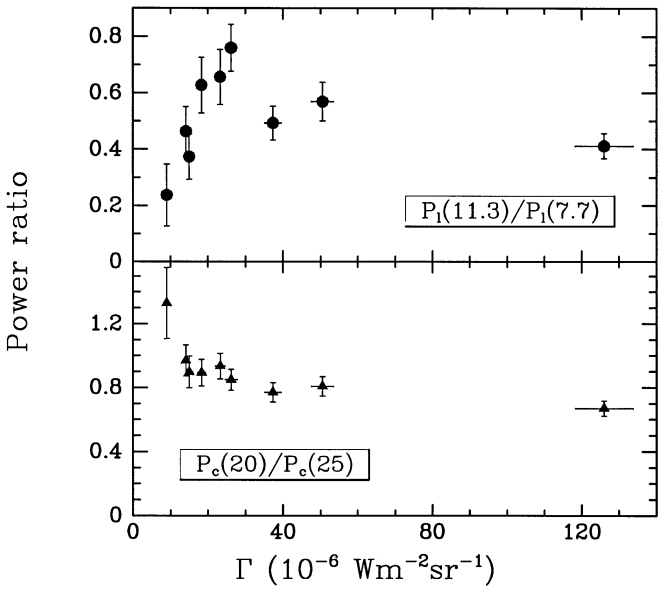

Fig. 5. Upper panel: $P_l(11.3)/P_l(7.7)$ as a function of Γ; **lower panel**: variation of $P_c(20)/P_c(25)$

The possible decrease of $P_c(20)/P_c(25)$ (Fig. 5) when coming closer to the central star may be due to an increasing emission contribution of both the large grain and the very small grain component in the 25 μm filter band. Model calculations by Désert et al. (1990) show a mild decrease similar to that observed in Fig. 5 for the ratio I_{12}/I_{25} as a result of the same mechanism. Refined model calculations should yield quantitative predictions for $P_c(20)/P_c(25)$. However, the presence of a discrete emission feature in the 20 μm band cannot be ruled out.

The 7.7 and 11.3 μm emission features become weaker relative to Γ when Γ decreases (Fig. 3). The fraction of total power in the two features relative to Γ is about 50% at position 9 and drops to less than 20% at position 1 which is about 0.5 pc from the exciting B3 star HD200775 (cf. Fig. 1). This suggests that the two PAH features are not the main emission components in the 5-15 μm range at the edge of the nebula. It is unclear to us how the trend extrapolates to the diffuse ISM where the radiation field is even weaker.

The ratio $P_l(11.3)/P_l(7.7)$ varies as a function of Γ but the relationship is not straightforward (Fig. 5). Assuming that the ISOPHOT 11.3 μm filter samples emission from solo out-of-plane bending modes (11.0-11.6 μm), our observation suggests that the amount of solo H sites changes relative to the amount of CC stretching sites which give rise to the 7.7 μm emission feature. In addition, the variation can be due to a varying ionization degree of the PAH molecules at the different positions investigated, with relatively more 7.7 μm emission at higher Γ (Joblin et al, 1996).

The clear rise of the 11.5 μm continuum towards the outer parts of the nebula as opposed to the constancy of $P_c(7.3)/\Gamma$ and $P_c(20)/\Gamma$ (Fig. 4) indicates that there must be an additional emission component in the 11.5 μm filter band. As the PHT-S spectrum (Fig. 2) does not hint to any other emission features in the 9-11.6 μm range of the 11.5 μm filter, we conclude that the other emission component should be relatively narrow and residing in the remaining 11.5-15 μm range. A possible explanation for this increasing emission component is an increase in the hydrogenation of the PAH molecules with increasing distance from the central star. Hydrogenation increases the amount of duo and trio H sites in PAH molecules which do not emit at 11.3 μm but do emit in the wavelength range 11.6-13.3 μm. This offers a natural explanation for the observed decrease of $P_l(11.3)/P_l(7.7)$ towards the edge of the nebula. A 12.7 μm emission feature and the underlying plateau related to this mechanism was observed for the first time by Cohen et al. (1985).

Acknowledgements. The ISOPHOT instrument was funded by the Deutsche Argentur für Raumfahrtangelegenheiten and the Max Planck Gesellschaft. The ISOPHOT data were reduced using PIA, a joint development by the ESA Astrophysics Division and the ISOPHOT consortium led by the Max Planck Institute for Astronomy, Heidelberg.

References

Casey S.C. 1991, ApJ 371, 183
Cohen M., Tielens A.G.G.M., Allamandola L.J. 1985, ApJL 299, 93
Désert, F,-X, Boulanger, F., Puget, J.L. 1990, A&A 237, 215
Joblin C., Tielens A.G.G.M., Geballe T.R., Wooden D.H. 1996, ApJL 460, 119
Klaas U., Krüger H., Heinrichsen I., Heske, A. Laureijs, R.J. 1994, ISOPHOT Observer's Manual, version 3.1.
Léger A., d'Hendecourt L., Defourneau D. 1989, A&A 216, 148
Lemke et al. 1996, A&A *this issue*
Puget J.L, Léger A. 1989, ARA&A 27, 161
Sellgren K. 1984, ApJ 277, 623
Sellgren K., Bregman J.D., Werner M.W., Wooden D.H. 1985, ApJ 299, 416